
Rethinking the Openness of CLIP

Shuhuai Ren¹, Lei Li¹, Xuancheng Ren¹, Guangxiang Zhao¹, Xu Sun^{1,2}

¹MOE Key Lab of Computational Linguistics, School of Computer Science, Peking University

²Center for Data Science, Peking University

{shuhuai_ren, lilei}@stu.pku.edu.cn

{renxc, zhaoguangxiang, xusun}@pku.edu.cn

Abstract

Contrastive Language-Image Pre-training (CLIP) has demonstrated great potential in realizing open-vocabulary image classification in a matching style, because of its holistic use of natural language supervision that covers unconstrained real-world visual concepts. However, it is, in turn, also difficult to evaluate and analyze the openness of CLIP-like models, since they are in theory open to any vocabulary but the actual accuracy varies. To address the insufficiency of conventional studies on openness, we resort to an incremental view and define the *extensibility*, which essentially approximates the model’s ability to deal with new visual concepts, by evaluating openness through vocabulary expansions. Our evaluation based on extensibility shows that CLIP-like models are hardly truly open and their performances degrade as the vocabulary expands to different degrees. Further analysis reveals that the over-estimation of openness is not because CLIP-like models fail to capture the general similarity of image and text features of novel visual concepts, but because of the confusion among competing text features, that is, they are not *stable* with respect to the vocabulary. In light of this, we propose to improve the openness of CLIP from the perspective of feature space by enforcing the distinguishability of text features. Our method retrieves relevant texts from the pre-training corpus to enhance prompts for inference, which boosts the extensibility and stability of CLIP even without fine-tuning.

1 Introduction

Deep neural networks have achieved remarkable success in visual recognition [6, 14, 28], which requests identifying the correct class of a target image from its potential classes. However, traditional visual recognition tasks, benchmarks, models, and learning algorithms are defined in a closed world [34, 20]. They cut a finite subset from the myriad visual categories in the real world and keep it fixed during training and inference, which limits their utility when the recognition target is updated dynamically. In contrast to the closed and static setting, a more realistic scenario for vision applications is *open world recognition* [34, 1, 2], where all existing visual concepts in the real world can become the potential class for a given input image. More importantly, in many applications like medical diagnosis [29] and video surveillance [15] etc., the target classes corresponding to input images will expand according to actual needs, which cannot be predefined either.

Faced with this challenging open-world recognition problem, traditional classifiers and algorithms have struggled, as they only learn to discriminate limited classes in a predefined closed set, and cannot adapt to the scaling of target classes. However, the emergence of Contrastive Language-Image Pre-training (CLIP) [28] and its *open vocabulary learning* paradigm has reversed this situation. CLIP models visual recognition as a task of image-text matching rather than the classic image classification. During inference, it devises a textual prompt like “a photo of a [CLASS]”, where the class token can be replaced by any potential class name from a vocabulary. The prompt-formed class description

with the highest similarity to the input image is predicted as the target class. This modeling paradigm makes CLIP *operationally* suitable for open tasks in the real world. When input images and the target classes change, CLIP can still conduct zero-shot inference by adaptively adjusting the names of potential classes in the vocabulary and then modifying the corresponding class descriptions for matching, sparing re-training the entire model on new data like the traditional classification-based methods. Nevertheless, contrary to the note “*CLIP has a wide range of capabilities due to its ability to carry out arbitrary image classification tasks*” in [28], previous evaluation of CLIP is still limited in the closed set, leaving its actual performance on open tasks in shadow.

In this work, we rethink openness, the intriguing but under-explored property of CLIP, and present a protocol for evaluating the openness of CLIP-like models [28, 23, 24, 38, 42] from an incremental view. Specifically, we define *extensibility*, which essentially approximates the models’s ability in dealing with new visual concepts through vocabulary expansion. Our experimental results based on extensibility show that CLIP and its variants have a significant drop in accuracy, e.g., 12.9% of CLIP (RN101) on CIFAR100 as the vocabulary size expands from 5 to 100, indicating that the limited zero-shot capability of CLIP-like models is not sufficient to support its deployment in the open world. Different from previous openness-related work, we focus on analyzing how the new class descriptions introduced with vocabulary expansion affect the *stability* of classification on the old input images. Our investigation reveals that the small margin between text features of different classes leads to the prediction shift. To improve the distinguishability of text features and the semantic alignment between images and their textual description, we propose a non-parametric method named Retrieval-enhanced Prompt Engineering (REPE), which retrieves relevant captions from pre-training corpus to enhance prompts for inference.

To summarize, our contribution is three-fold: **(1)** To our best knowledge, we are the first to investigate the openness of CLIP, for which we design the evaluation protocol and two indicators of extensibility and stability. Through an analysis of the prediction shift during vocabulary expansion, we find that the performance of CLIP is greatly reduced by adding a small number of adversarial non-target classes, exposing the huge risk of its deployment in the open world. **(2)** We further dissect the feature space of CLIP from the perspectives of representation alignment and uniformity, observing that the uniformity of the textual space is critical for better extensibility. **(3)** We propose a simple yet effective method, REPE, to improve the extensibility and stability of CLIP without fine-tuning.

2 Openness, extensibility, and stability

In this section, we first review CLIP’s visual recognition paradigm based on image-text matching, and then demonstrate how it realizes open-vocabulary image classification in theory by vocabulary expansion (§ 2.1). To quantify the actual performance of CLIP-like models as the vocabulary expands to various degrees, we define the metric of extensibility and propose an evaluation protocol (§ 2.2). The experimental results and further analysis reveal that the predictions of CLIP are unstable and prone to drift to the competing class descriptions that are newly introduced as the vocabulary expands, which limits its extensibility and leaves a huge security risk when deployed in real-world applications (§ 2.3).

2.1 Openness of CLIP

The seek for an intrinsically open mechanism of visual recognition has always been a shared goal in the computer vision community [34, 11, 1]. A highly open scenario with varied and dynamic needs requires models to maintain flexibility to cope with the scaling of *target classes*, i.e., all the ground-truth categories of input images. CLIP [28] takes a big step towards this goal by modeling visual recognition as an image-text matching task with large scale contrastive pre-training. Formally, let f be the CLIP model, it takes an image \mathbf{x} and a vocabulary $\mathcal{V} = \{w_i\}$ of the potential class names w_i as inputs, and outputs the predicted label \hat{y} of the target image as:

$$\begin{aligned} \hat{y} &= f(\mathbf{x}, \mathcal{V}) = \arg \max_i P(y = i | \mathbf{x}) \\ &= \arg \max_i \frac{\exp(\text{sim}(f_T(\mathbf{t}_i), f_I(\mathbf{x})))}{\sum_{j=1}^{|\mathcal{V}|} \exp(\text{sim}(f_T(\mathbf{t}_j), f_I(\mathbf{x})))}, \end{aligned} \tag{1}$$

where \mathbf{t}_i is the textual description of the class name w_i in a prompt format, e.g., “a photo of a w_i ”, $\text{sim}(\cdot, \cdot)$ denotes cosine similarity, f_T and f_I is the text and image encoder in CLIP, respectively. Such a modeling paradigm can realize the open-world image classification in theory by extending the *target vocabulary*, i.e., the vocabulary of target classes, to arbitrary degrees. However, in most previous work [28, 23, 24, 38, 42], CLIP is evaluated with a fixed target vocabulary $\mathcal{V}^{(T)}$ of the corresponding dataset $\mathcal{D}^{(T)}$, where the number of target classes remains unchanged in inference:

$$\text{Acc}(\mathcal{V}^{(T)}) = \frac{1}{|\mathcal{D}^{(T)}|} \sum_{(\mathbf{x}, y) \in \mathcal{D}^{(T)}} \mathbb{I}(f(\mathbf{x}, \mathcal{V}^{(T)}) = y). \quad (2)$$

Here, $|\mathcal{D}^{(T)}|$ denotes the number of samples in the dataset, and $\mathbb{I}(\cdot)$ is the indicator function. We argue that this vanilla evaluation setting is insufficient for the open recognition tasks with CLIP, as it does not explicitly and systematically model the dynamics of vocabulary expansion during inference, and thus cannot reflect the actual openness of CLIP in the face of real-life class scaling.

2.2 Quantifying extensibility of CLIP for the open world

To quantify the model’s capability in dealing with newly emerged target classes, we propose an evaluation protocol and define a metric of extensibility based on vocabulary expansion. Concretely, we incrementally expand the vocabulary $\mathcal{V}^{(T)}$ in Eq. 2 by introducing new target classes and the associated input images, then evaluate the accuracy after each vocabulary expansion. These values of accuracy measure the dynamic performance of the model as the openness gradually increases, and their expected average is defined as the model’s extensibility. In practice, we achieve this expansion by incrementally unioning N disjoint target vocabularies ¹:

Definition 2.1 (Extensibility). Given N disjoint target vocabularies $\{\mathcal{V}_1^{(T)}, \dots, \mathcal{V}_N^{(T)}\}$ and their full permutation \mathcal{S}_N , we denote s_i as the i^{th} target vocabulary $\mathcal{V}_{s_i}^{(T)}$ in a permutation $s \in \mathcal{S}_N$. When we union the $(i+1)^{\text{th}}$ vocabulary $\mathcal{V}_{s_{i+1}}^{(T)}$ with the previous i vocabularies $\mathcal{V}_{s_1}^{(T)} \cup \dots \cup \mathcal{V}_{s_i}^{(T)}$, we achieve a vocabulary expansion. The extensibility refers to the averaged classification accuracy across N incremental expansions as i increases from 1 to N :

$$\text{Acc-E} = \mathbb{E}_{s \in \mathcal{S}_N} \frac{1}{N} \sum_{i=1}^N \text{Acc}(\mathcal{V}_{s_1}^{(T)} \cup \dots \cup \mathcal{V}_{s_i}^{(T)}). \quad (3)$$

Experimental settings We evaluate the extensibility of CLIP and its variants, including DeCLIP [23], SLIP [24], Prompt Ensemble [28], CoOp [42], on the CIFAR100 [22] and ImageNet [6] datasets. Non-matching methods [10, 41, 36] like linear probing, etc., are NOT included since they require training a classifier with finite class vectors, and thus are not suitable for open tasks in operation. To construct the vocabulary, we leverage the underlying superclass-class hierarchical structure of the two datasets, and group the classes belonging to the same superclass into a vocabulary. The superclass-class structure of CIFAR100 and ImageNet is specified by [22] and BREEDS [32], respectively. There are 20 vocabularies in CIFAR100, each with 5 classes. For ImageNet, we utilize two superclass-class structures: Entity13 and Living17. The former has 13 vocabularies, each with 20 classes, while the latter has 17 vocabularies, each with 4 classes. ² Tables in the Appendix A list all the vocabularies in the two datasets. For each dataset, we calculate Acc-C, the averaged classification accuracy across all single vocabularies, based on Eq. 2:

$$\text{Acc-C} = \frac{1}{N} \sum_{i=1}^N \text{Acc}(\mathcal{V}_i^{(T)}). \quad (4)$$

It represents the original model performance on closed vocabularies. To calculate the expectation in Acc-E, we sample $100 \times N$ permutations of N vocabularies for each dataset and take the average.

Results As shown in Table 1, all models exhibit a clear drop in performance as the openness of tasks increases. For example, on CIFAR100, compared with averaged accuracy (Acc-C) across the 20 individual vocabulary with a size of 5, the accuracy (Acc-E) of CLIP (RN101) decreased by

¹Since $\mathcal{V}^{(T)}$ is bound with $\mathcal{D}^{(T)}$ in Eq. 2, target vocabulary expansion implies expanding $\mathcal{D}^{(T)}$ (including input images and their labels) at the same time, which we omit for brevity.

²Hence, the N in Def. 2.1 for CIFAR100, ImageNet (Entity13) and (Living17) is 20, 13 and 17, respectively.

Table 1: Extensibility and stability of CLIP and its variants on CIFAR100 and ImageNet datasets (BREEDS benchmark). Δ refers to the decline of Acc-E/Acc-S (%) compared to Acc-C (%). PE denotes Prompt Ensemble. CoOp is prompt-tuned on all classes with 16 shots.

Model	CIFAR100					ImageNet (Entity13)					ImageNet (Living17)				
	Acc-C	Extensibility		Stability		Acc-C	Extensibility		Stability		Acc-C	Extensibility		Stability	
		Acc-E	Δ	Acc-S	Δ		Acc-E	Δ	Acc-S	Δ		Acc-E	Δ	Acc-S	Δ
CLIP (RN101)	68.3	55.4	-12.9	54.9	-13.4	80.4	77.4	-3.0	77.3	-3.1	77.6	74.5	-2.9	74.4	-3.0
CLIP (ViT-B/32)	78.0	69.6	-8.4	68.9	-9.1	80.8	78.0	-2.8	77.8	-3.0	78.0	74.4	-3.6	75.0	-3.0
CLIP (ViT-B/16)	79.7	72.6	-7.1	72.0	-7.7	83.5	81.1	-2.4	81.0	-2.5	79.5	77.9	-1.6	77.6	-1.9
SLIP (ViT-B/16)	63.9	51.1	-12.8	50.4	-13.5	65.7	62.3	-3.4	62.0	-3.7	65.7	62.6	-3.1	62.5	-3.2
DeCLIP (ViT-B/32)	78.7	70.8	-7.9	70.4	-8.3	81.9	79.2	-2.7	79.1	-2.8	82.1	80.2	-1.9	80.0	-2.1
PE (ViT-B/32)	78.3	70.3	-8.0	69.9	-8.4	81.9	79.4	-2.5	79.2	-2.7	78.7	76.0	-2.7	75.8	-2.9
PE (ViT-B/16)	79.6	72.6	-7.0	72.0	-7.6	85.3	83.2	-2.1	83.1	-2.2	79.6	78.2	-1.4	78.0	-1.6
CoOp (ViT-B/16)	83.6	76.9	-6.7	76.7	-6.9	87.5	85.3	-2.2	85.5	-2.0	82.7	82.6	-0.1	81.3	-1.4

12.9% after the vocabulary is gradually expanded by a factor of 20, showing the weak extensibility of CLIP. Figure 10 in Appendix C shows the Acc-E for several trials on CIFAR100 as new vocabularies are merged incrementally. The falling lines indicate that the model is either performing poorly on the new input images or that some images that were correctly identified before are misclassified after introducing the new classes. These results demonstrate that **CLIP-like models are far from satisfactory for open visual recognition tasks**. Appendix B provides results of expansion at the dataset level where the expanded vocabularies are from different datasets. The performance of CLIP-like models drops even more dramatically on generic dataset expansion. Besides, there are some interesting findings: (1) From the perspective of pre-training, introducing a strong vision backbone (ViT [7] v.s. ResNet [14]), widespread supervision (DeCLIP [23] v.s. CLIP), and more pre-training data (CLIP v.s. SLIP [24]) can improve the extensibility of models on open tasks. (2) During inference, the performance of CLIP can be boosted by ensembling different prompts [28]. (3) CoOp [42] that conducts prompt tuning on all classes of CIFAR100 and ImageNet yields the most extensible results. However, the prompt tuning method utilizes the predefined category information and training data in the target dataset, which cannot be transferred to real-life open tasks.

2.3 Stability during vocabulary expansion

As the vocabulary expansion introduces new classes incrementally, some input images belonging to the previous vocabulary will be incorrectly predicted as new classes, which leads to an accuracy drop and the poor extensibility. To analyze the prediction stability of CLIP during vocabulary expansion, we introduce the *non-target classes* that do NOT have the associated input images, and define classification accuracy on the target vocabulary $\mathcal{V}^{(T)}$ conditioning on the potential vocabulary $\mathcal{V}^{(T)} \cup \mathcal{V}^{(NT)}$:

$$\text{Acc} \left(\mathcal{V}^{(T)} \middle| \mathcal{V}^{(T)} \cup \mathcal{V}^{(NT)} \right) = \frac{1}{|\mathcal{D}^{(T)}|} \sum_{(\mathbf{x}, y) \in \mathcal{D}^{(T)}} \mathbb{I} \left(f \left(\mathbf{x}, \mathcal{V}^{(T)} \cup \mathcal{V}^{(NT)} \right) = y \right), \quad (5)$$

where $\mathcal{V}^{(NT)}$ is the *non-target vocabulary*, i.e., the vocabulary of non-target classes. Figure 1 gives an illustration of the conditional accuracy of CLIP on open tasks. In Eq. 5, the categories of input images are limited to the target vocabulary $((\mathbf{x}, y) \in \mathcal{D}^{(T)})$, but CLIP is asked to distinguish all categories from the potential vocabulary during inference. In other words, compared to the traditional closed-set classification, CLIP is supposed to reject all the negative categories from $\mathcal{V}^{(NT)}$. The model is required to distinguish visual concepts stably and robustly, rather than making wrong predictions in the presence of other distractors. Based on Eq. 5, we define the stability of CLIP in the open task:

Definition 2.2 (Stability). Given a target vocabulary $\mathcal{V}^{(T)}$ and N non-target vocabularies $\{\mathcal{V}_1^{(NT)}, \dots, \mathcal{V}_N^{(NT)}\}$, we denote \mathcal{S}_N as their full permutation and s_i as the i^{th} vocabulary $\mathcal{V}_{s_i}^{(NT)}$ in a permutation $s \in \mathcal{S}_N$, the **local stability** measures the averaged classification accuracy of CLIP on the given target vocabulary when non-target vocabularies are extended incrementally:

$$\text{Acc-}\tilde{\text{S}} \left(\mathcal{V}^{(T)}, \mathcal{V}^{(NT)} \right) = \mathbb{E}_{s \in \mathcal{S}_N} \frac{1}{N} \sum_{i=1}^N \text{Acc} \left(\mathcal{V}^{(T)} \middle| \mathcal{V}^{(T)} \cup \left(\mathcal{V}_{s_1}^{(NT)} \cup \dots \cup \mathcal{V}_{s_i}^{(NT)} \right) \right). \quad (6)$$

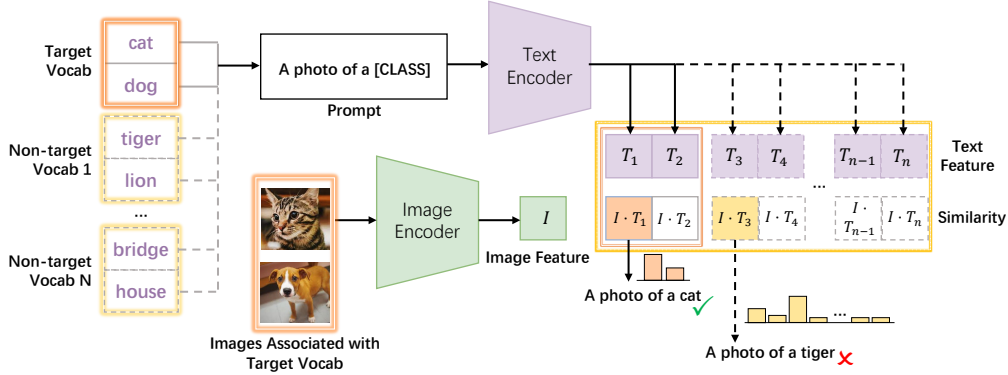


Figure 1: Conditional accuracy of CLIP with non-target vocabularies (Eq. 5). Misclassification occurs when the model is asked to recognize target classes from more potential classes.

As Eq. 6 only reflects the local stability with respect to a single target vocabulary, we further design the **general stability** as an average of local stability over a set of target vocabularies to alleviate the impact of data distribution and vocabulary sampling on the evaluation of model capability. Specifically, given M vocabularies $\{\mathcal{V}_1, \dots, \mathcal{V}_M\}$, we regard each vocabulary \mathcal{V}_i as the target vocabulary $\mathcal{V}^{(T)}$ and the rest $\mathcal{V}_{\neq i}$ as the non-target vocabularies $\mathcal{V}^{(NT)}$, and then formulate the general stability as:

$$\text{Acc-S} = \frac{1}{M} \sum_{i=1}^M \text{Acc-}\tilde{\text{S}}(\mathcal{V}_i, \mathcal{V}_{\neq i}). \quad (7)$$

Experimental settings and results The models and datasets adopted for evaluation are consistent with that in § 2.2. For the calculation of stability, take CIFAR100 with $M = 20$ vocabularies as an example, we treat each vocabulary as the target vocabulary and the rest are treated as the non-target vocabularies for Eq. 7. To calculate the expectation in Eq. 6, we sample 100 permutations for $N = 19$ non-target vocabularies and report the averaged scores.

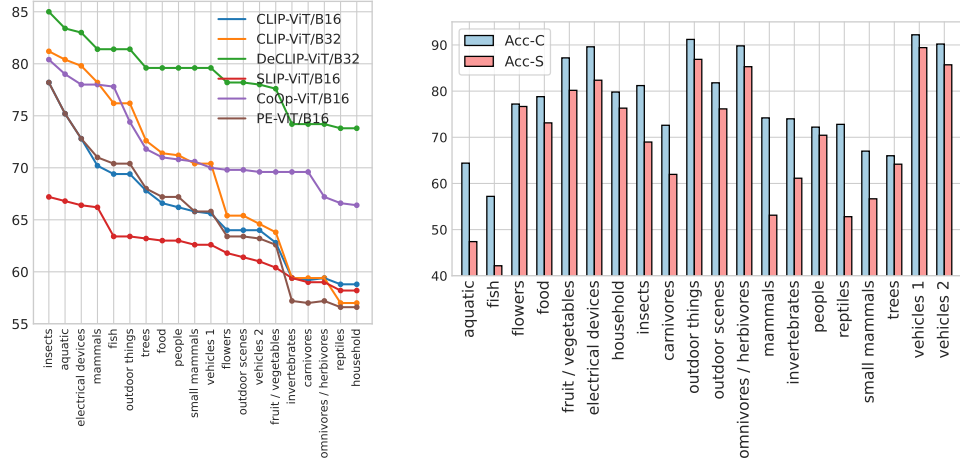
Table 1 demonstrates the stability of CLIP-like models. On CIFAR100, the Acc-S of CLIP (RN101) decreased by 13.4% after adding 95 intrusive non-target classes. Figure 2a shows Acc-S on CIFAR100 during non-target vocabulary expansion. CLIP (ViT-B/32) achieves an accuracy of 81.2% on the closed target vocabulary of *Insects*. However, when the remaining 19 non-target vocabularies are incorporated and the model is required to recognize the 5 target classes in *Insects* from 100 potential classes, the accuracy sharply drops to 57.0%. The decrease of Acc-S brought by each introduction of non-target vocabulary indicates that more images from *Insects* are incorrectly classified into the new non-target vocabulary by models. Figure 2b demonstrates the difference between Acc-C and Acc-S for each target vocabulary. When *Medium-sized Mammals* is treated as the target vocabulary, CLIP (ViT-B/32) is most easily interfered with by the non-target vocabularies, with a 21.08% performance drop. It suggests that **the unstable predictions when new categories are introduced lead to the poor extensibility of CLIP**. Besides, we notice that CLIP performs stably on groups like *Flowers*, where its Acc-S only declines by 0.53% compared to Acc-C. The different behaviors of different groups, e.g., CLIP performs stably on *Flowers* while is brittle for *Medium-sized Mammals*, indicating that **the stability is also influenced by the inherent property of the image categories**.

2.3.1 Adversarial non-target vocabulary

In order to explore the lower bound of the stability of CLIP, we define the *adversarial non-target vocabulary* $\mathcal{V}^{(ANT)}$ as the non-target vocabulary that reduces Acc-S the most:

$$\mathcal{V}^{(ANT)} = \min_{\mathcal{V}^{(NT)}} \text{Acc}(\mathcal{V}^{(T)} | \mathcal{V}^{(T)} \cup \mathcal{V}^{(NT)}). \quad (8)$$

To build $\mathcal{V}^{(ANT)}$, we refer to the method of adversarial examples generation in the Natural Language Processing field [30] to traverse the words in a large vocabulary, e.g., the vocabulary of nouns in WordNet [9], which are regarded as non-target classes in order to calculate Acc-S, and then take the most confusing words to form the adversarial non-target vocabulary.



(a) Acc-S drops as non-target vocabulary extends (*Insects* as target vocabulary). (b) Difference between Acc-C and Acc-S of CLIP (ViT-B/32) on different groups.

Figure 2: Acc-C and Acc-S (%) of CLIP and its variants on CIFAR100. The horizontal axis represents the extended non-target vocabularies in order. PE refers to Prompt Ensemble.

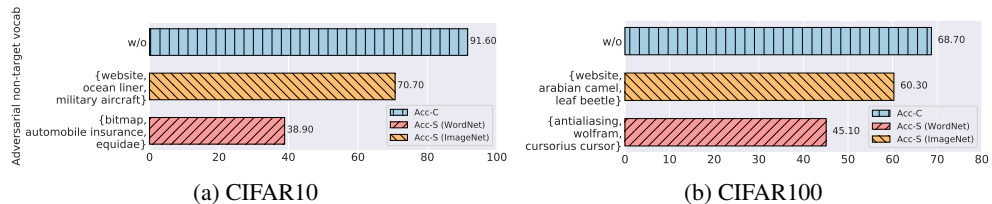


Figure 3: Adversarial non-target vocabulary and the corresponding Acc-S on CIFAR datasets. Adding 3 non-target classes into the candidates leads to severe performance deterioration, revealing the vulnerability of CLIP when faced with malicious vocabulary.

We constrain the size of $\mathcal{V}^{(ANT)}$ to 3. Results in Figure 3 illustrate the performance with nouns in WordNet and class names in ImageNet as the candidate vocabulary, respectively. First, we observe a clear performance degradation on both datasets under adversarial attack, e.g., adding *bitmap*, *automobile insurance* and *equidae* leads to an absolute 52.7% accuracy drop on CIFAR10. Besides, we find that the selected adversarial words are much less concrete than common visual concepts like *Flower*, indicating the potential reason behind is the poor semantic modeling of CLIP on those objects with higher abstraction levels. This investigation reveals that **CLIP is vulnerable when facing malicious non-target vocabulary**, and we hope future work may pay more attention to the robustness of CLIP under open recognition tasks.

3 Dissecting and improving the extensibility of CLIP

Our experimental results in § 2 expose the unsatisfying performance of CLIP on open tasks, especially its unstable prediction with respect to the vocabulary expansion. In this section, we dive into the representation space of CLIP to find the key to understanding and improving its extensibility. We first point out that the small margin between positive and negative class descriptions leads to the prediction shift when competing text features appear, which thus limits the stability of CLIP (§ 3.1). Further, we investigate the representation space of CLIP-like models via two metrics of inter-modal alignment and intra-modal uniformity. The results show that enforcing the distinguishability of text features enlarges the margin and makes models scale more stably (§ 3.2). In response, we propose a *non-parametric* method named Retrieval-enhanced Prompt Engineering (REPE), which boosts the performance of CLIP even without fine-tuning (§ 3.3).

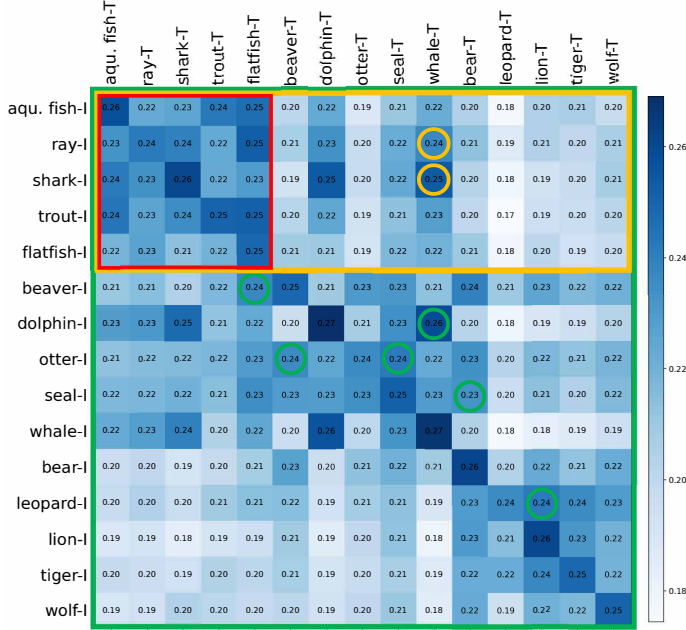


Figure 4: Averaged cosine similarity between image (-I) and text (-T) features of CLIP (ViT-B/32) on CIFAR100. The expansion from the red box to the green box (diagonal) and the yellow box (horizontal) refer to the calculation of extensibility and stability, respectively. The circle represents that more than 15 new wrong predictions have occurred after adding this class.

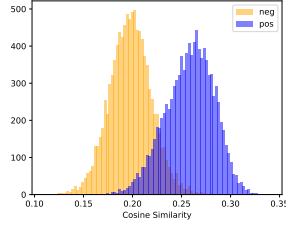


Figure 5: Cosine similarity histogram of positive (pos) and negative (neg) image-text pairs with large overlap.

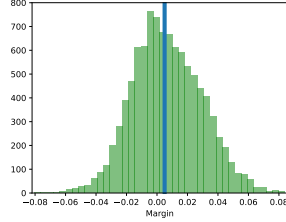


Figure 6: Margin distribution of similarity scores, which are centered around zero with a median value of .005 (the blue vertical line). It indicates that the predictions can be easily inverted with competing classes appearing.

3.1 Small margin limits the stability of CLIP

Since CLIP formalizes the visual recognition as an image-text matching task (Eq. 1), each text feature of the prompt-formed class name corresponds to the class vector in traditional classifiers, and the image-text similarity scores are thus analogous to the logits in classification. Ideally, no matter how the vocabulary expands, for an image, the similarity of the positive pair, i.e., the image with the text specifying the ground-truth class, should be higher than those of the negative pairs, i.e., the image with the texts specifying other classes, to ensure the correct prediction of CLIP on open tasks. In other words, the *margin* [18] between positive and the largest negative similarity is a direct contributing factor to the stability.

Unfortunately, the similarity and margin distribution of CLIP does not meet our expectations. Figure 4 illustrates the averaged cosine similarity between image and text features of CLIP (ViT-B/32) on 15 classes of CIFAR100. Similarity over the intact dataset is in Appendix D. The diagonal elements represent the similarity of the positive image-text pairs, while the others represent that of the negative ones. The cosine similarity of image-text pairs is very low, with an average of 0.20. This number is only 0.26 even for the positive pairs. Besides, the similarities of positive and negative pairs are very close, indicating the low distinguishability between different classes. As shown in Figure 5, the similarity histogram of positive and negative pairs has a large overlap. Its margin in Figure 6 is clustered around zero, leaving the prediction of models at risk of being reversed to the new non-target classes. For example, as the vocabulary extends from the red box to the green box (diagonal) or the yellow box (horizontal) in Figure 4, more deceptive classes (circle) with negative margin are added, which leads to the prediction shift. Particularly, the classes belonging to the same vocabulary³ have higher similarity and smaller margin, which is more likely to be confused with each other.

³Every 5 adjacent classes in Figure 4 constitute a vocabulary (superclass), see Table 2 in Appendix A

3.2 Inter-modal alignment and intra-modal uniformity ground the margin

The results in § 3.1 raise a natural question: what vision-and-language feature distribution can maintain a large margin between different classes so that the model can scale stably in the open world? Here we present two properties of the ideal feature space: First, the text feature of a class name is supposed to stay close to the features of the images it describes, promoting the similarity of positive pairs. Second, intra-modal features, especially the textual features should be uniformly distributed to preserve maximal information and make the descriptions of competing categories more distinguishable. Accordingly, we introduce *inter-modal alignment* and *intra-modal uniformity*, two metrics to measure the quality of representations in contrastive learning [35] for the vision-and-language domain. Inter-modal alignment calculates the expected distance between features of positive image-text pairs p_{pos} :

$$\ell_{\text{align}} \triangleq \mathbb{E}_{(\mathbf{x}, \mathbf{t}) \sim p_{\text{pos}}} \|f_I(\mathbf{x}) - f_T(\mathbf{t})\|^2, \tag{9}$$

while intra-modal uniformity measures how well the image or text features are uniformly distributed:

$$\begin{aligned} \ell_{\text{uniform}} &\triangleq \ell_{\text{uniform-I}} + \ell_{\text{uniform-T}} \\ &\triangleq \log \mathbb{E}_{\mathbf{x}_i, \mathbf{x}_j \stackrel{i.i.d.}{\sim} p_{\text{data-I}}} e^{-2\|f_I(\mathbf{x}_i) - f_I(\mathbf{x}_j)\|^2} + \log \mathbb{E}_{\mathbf{t}_i, \mathbf{t}_j \stackrel{i.i.d.}{\sim} p_{\text{data-T}}} e^{-2\|f_T(\mathbf{t}_i) - f_T(\mathbf{t}_j)\|^2}, \end{aligned} \tag{10}$$

where $p_{\text{data-I}}$ and $p_{\text{data-T}}$ denotes the image and text data distribution, respectively. Figure 7 and Table 6 in Appendix E provide quantified loss of alignment and uniformity. CLIP with only cross-modal contrastive learning results in poor intra-modal uniformity ($\ell_{\text{uniform}} > -2.0$), especially on the text side. Introducing intra-modal contrastive learning like SLIP [24] and DeCLIP [23] in pre-training can force both image and text features separate better from classes, reducing ℓ_{uniform} to below -4.5 . As for the prompt tuning [42] method (CoOp), it achieves better ℓ_{align} of 1.4 compared to CLIP (1.5) and the lowest $\ell_{\text{uniform-T}}$ of -3.2 . According to the visualization via Multidimensional Scaling (MDS) [3] in Figure 8, the optimization trajectory of prompts is towards the cluster center of the corresponding image features, while dispersing the position of the prompt features, which improves both text uniformity and inter-modal alignment, achieving the best extensibility.

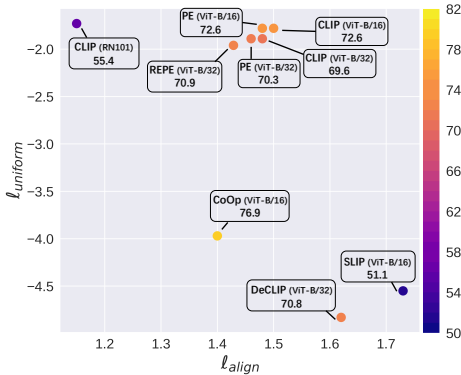


Figure 7: ℓ_{align} and ℓ_{uniform} of CLIP-like models. For both two metrics, lower numbers are better. The color of points and numbers denote the extensibility performance (Acc-E) on CIFAR100 (higher is better).

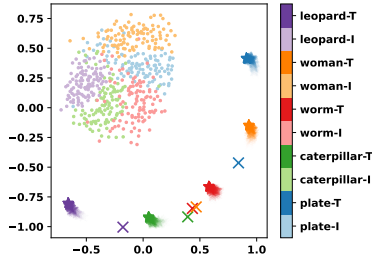


Figure 8: Representation visualization of CLIP and CoOp (ViT-B/16). The five classes with different colors are from CIFAR100. ● refers to image features (-I), while × and ★ refers to text features (-T) of CLIP and CoOp, respectively. The color of ★ from transparent to opaque indicates the optimization trajectory during the CoOp prompt-tuning process.

3.3 Methodology: Retrieval-enhanced prompt engineering (REPE)

In light of the previous investigations, we propose a simple but effective method named Retrieval-enhanced Prompt Engineering (REPE) to enforce the distinguishability of text features and the semantic alignment [4, 31]. We assume that the original text prompt like “a photo of a [CLASS]” is not optimal, as the same context in the prompt cannot provide holistic and diverse semantics modeling for different visual categories [43]. To remedy this, we propose to retrieve the captions from pre-training dataset as a prompt ensemble. Specifically, for each class description based on the original prompt, we utilize CLIP to recall the most similar images from the pre-training dataset to further obtain their corresponding captions. The retrieved captions without class name appearance

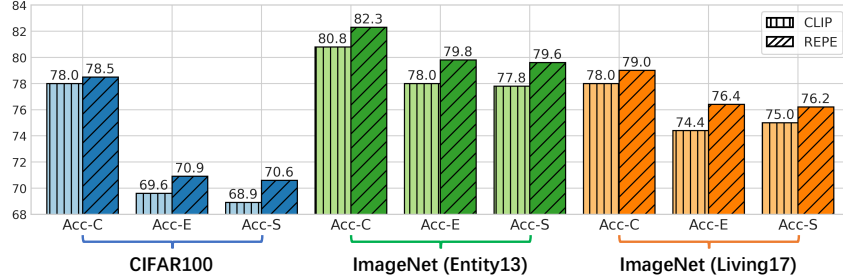


Figure 9: Extensibility and stability of our retrieval-enhanced prompt engineering (REPE) on CIFAR100 and ImageNet datasets. The vision backbone of both CLIP and REPE is ViT-B/32.

are then filtered out, finally resulting in K captions. Appendix F shows the instances of the retrieved captions. They share the same target of interest with the original prompt but provide the context in which the class name is located and thus have richer semantics. After that, we encode the retrieved captions and conduct a mean pooling operation among them. The final textual representation is

$$f_T^{\text{REPE}}(\mathbf{t}_i) = (1 - \lambda)f_T(\mathbf{t}_i) + \lambda \frac{1}{K} \sum_j^K f_T(\mathbf{rt}_{ij}) \quad (11)$$

where \mathbf{rt}_{ij} is the j^{th} retrieved caption for class i , λ is a weighting factor and is adjusted on the validation set. The ensemble text representation $f_T^{\text{REPE}}(\mathbf{t}_i)$ is then adopted as the class anchor for conducting the image classification. The text representation for each class is thus shifted towards the representative captions for the target image class in the pre-training dataset, which alleviates the semantic inconsistency between pre-training and inference.

Experiments We retrieve the images and captions from CC12M [5], a subset of the pre-training dataset of CLIP. The retrieval is effectively implemented by using the FAISS framework [19], where millions of images and captions can be indexed and retrieved within several minutes. Figure 9 shows the results of retrieval-enhanced prompt engineering. The hyper-parameter K is 100. We find that on all the three datasets, REPE consistently improves the extensibility and stability of the original CLIP model by an average of 1.63%. We further evaluate the loss of text uniformity and inter-modal alignment for probing the quality of the enhanced representations. As shown in Figure 7, the former is effectively reduced from -0.85 to -1.01 and the latter is reduced from 1.50 to 1.43, verifying our proposal can improve the class anchor for better extensibility and the stability of original CLIP model. It is worth noting that compared to the method that requires computation-intensive pre-training procedure (DeCLIP and SLIP), and the prompt-tuning approach (CoOp) demands the access to the target dataset which can be unavailable for the real open-world recognition, our REPE is a lightweight framework for the zero-shot inference stage without either pre-training or fine-tuning.

4 Related work

Contrastive language-image pre-training and open-vocabulary learning Contrastive Language-Image Pre-training (CLIP) [28] introduces the paradigm of open-vocabulary learning, which enables learning transferable visual models from natural language supervision and makes visual recognition generalize in the wild [40, 13, 12]. It is pre-trained on web-scale collections of image-text pairs, learning tremendous visual concepts described by natural language with contrastive learning. During inference, it devises a prompt like “a photo of a [CLASS]”, where the class token is a placeholder for any potential class name from a vocabulary, and the prompt-formed class name with the highest similarity to the input image is predicted as the target class. Recent studies further improve CLIP by using more pre-training data [17], incorporating self-supervision [24], fine-grained supervision [38], and widespread supervision [23] to pre-training.

Open set and open-world visual recognition In traditional supervised learning, models are unable to acquire complete knowledge to cope with the novel input images encountered in inference. Therefore, the Open Set Recognition (OSR) [34, 11] has been proposed to require classifiers to

identify images that have not been introduced during training as “unknown”. The task can be formalized as one-vs-reset classification [34] or multi-class classification [16, 33]. Reconstruction-based algorithms [27, 39] are the recent prevalent methods for OSR. Furthermore, Open World Recognition (OWR) [1] raises higher demands that the model must incrementally learn and extend the multi-class classifier as the unknowns are labeled for new class learning.

Contrary to the above research, the CLIP-based Open-vocabulary Recognition (OVR) is unsupervised. We focus on the model performance on zero-shot inference, without training or fine-tuning on the target dataset. Appendix G provides a more detailed comparison of OSR, OWR, and OVR.

5 Conclusion

In this paper, we evaluate the extensibility of CLIP under open visual recognition settings, where the model is required to make accurate predictions with emerging classes and associated images. We find that the performance of CLIP-like models deteriorates seriously as the vocabulary expands, resulting in poor extensibility and stability for real open tasks. Further analysis shows that the reason behind this is the indistinguishable representations among competing text features. To remedy this, we propose REPE to enhance the textual representations with retrieved relevant descriptions of classes from the pre-training corpus. Experiments verify that REPE can boost the extensibility and stability even without pre-training and fine-tuning. We hope our work can facilitate future studies towards designing better architectures for the open recognition tasks.

References

- [1] Abhijit Bendale and Terrance E. Boult. Towards open world recognition. In *IEEE Conference on Computer Vision and Pattern Recognition, CVPR 2015, Boston, MA, USA, June 7-12, 2015*, pages 1893–1902. IEEE Computer Society, 2015.
- [2] Abhijit Bendale and Terrance E. Boult. Towards open set deep networks. In *2016 IEEE Conference on Computer Vision and Pattern Recognition, CVPR 2016, Las Vegas, NV, USA, June 27-30, 2016*, pages 1563–1572. IEEE Computer Society, 2016.
- [3] Ingwer Borg and Patrick J. F. Groenen. Modern multidimensional scaling: Theory and applications. *Journal of Educational Measurement*, 40:277–280, 1997.
- [4] Jize Cao, Zhe Gan, Yu Cheng, Licheng Yu, Yen-Chun Chen, and Jingjing Liu. Behind the scene: Revealing the secrets of pre-trained vision-and-language models. In *ECCV*, 2020.
- [5] Soravit Changpinyo, Piyush Kumar Sharma, Nan Ding, and Radu Soricut. Conceptual 12m: Pushing web-scale image-text pre-training to recognize long-tail visual concepts. *2021 IEEE/CVF Conference on Computer Vision and Pattern Recognition (CVPR)*, pages 3557–3567, 2021.
- [6] Jia Deng, Wei Dong, Richard Socher, Li-Jia Li, Kai Li, and Fei-Fei Li. Imagenet: A large-scale hierarchical image database. In *2009 IEEE Computer Society Conference on Computer Vision and Pattern Recognition (CVPR 2009), 20-25 June 2009, Miami, Florida, USA*, pages 248–255. IEEE Computer Society, 2009.
- [7] Alexey Dosovitskiy, Lucas Beyer, Alexander Kolesnikov, Dirk Weissenborn, Xiaohua Zhai, Thomas Unterthiner, Mostafa Dehghani, Matthias Minderer, Georg Heigold, Sylvain Gelly, Jakob Uszkoreit, and Neil Houlsby. An image is worth 16x16 words: Transformers for image recognition at scale. In *9th International Conference on Learning Representations, ICLR 2021, Virtual Event, Austria, May 3-7, 2021*. OpenReview.net, 2021.
- [8] Li Fei-Fei, Rob Fergus, and Pietro Perona. Learning generative visual models from few training examples: An incremental bayesian approach tested on 101 object categories. In *CVPR Workshops*, 2004.
- [9] Christiane D. Fellbaum. Wordnet : an electronic lexical database. *Language*, 76:706, 2000.
- [10] Peng Gao, Shijie Geng, Renrui Zhang, Teli Ma, Rongyao Fang, Yongfeng Zhang, Hongsheng Li, and Yu Jiao Qiao. Clip-adapter: Better vision-language models with feature adapters. *ArXiv*, abs/2110.04544, 2021.

- [11] Chuanxing Geng, Sheng-Jun Huang, and Songcan Chen. Recent advances in open set recognition: A survey. *IEEE Transactions on Pattern Analysis and Machine Intelligence*, 43:3614–3631, 2021.
- [12] Golnaz Ghiasi, Xiuye Gu, Yin Cui, and Tsung-Yi Lin. Open-vocabulary image segmentation. *ArXiv*, abs/2112.12143, 2021.
- [13] Xiuye Gu, Tsung-Yi Lin, Weicheng Kuo, and Yin Cui. Open-vocabulary object detection via vision and language knowledge distillation. In *International Conference on Learning Representations*, 2022.
- [14] Kaiming He, Xiangyu Zhang, Shaoqing Ren, and Jian Sun. Deep residual learning for image recognition. In *2016 IEEE Conference on Computer Vision and Pattern Recognition, CVPR 2016, Las Vegas, NV, USA, June 27-30, 2016*, pages 770–778. IEEE Computer Society, 2016.
- [15] Andrei De Souza Inácio, Matheus Gutoski, André Eugênio Lazzaretti, and Heitor Silvério Lopes. Osvidcap: A framework for the simultaneous recognition and description of concurrent actions in videos in an open-set scenario. *IEEE Access*, 9:137029–137041, 2021.
- [16] Lalit P. Jain, Walter J. Scheirer, and Terrance E. Boult. Multi-class open set recognition using probability of inclusion. In *ECCV*, 2014.
- [17] Chao Jia, Yinfei Yang, Ye Xia, Yi-Ting Chen, Zarana Parekh, Hieu Pham, Quoc V. Le, Yun-Hsuan Sung, Zhen Li, and Tom Duerig. Scaling up visual and vision-language representation learning with noisy text supervision. In Marina Meila and Tong Zhang, editors, *Proceedings of the 38th International Conference on Machine Learning, ICML 2021, 18-24 July 2021, Virtual Event*, volume 139 of *Proceedings of Machine Learning Research*, pages 4904–4916. PMLR, 2021.
- [18] Yiding Jiang, Dilip Krishnan, Hossein Mobahi, and Samy Bengio. Predicting the generalization gap in deep networks with margin distributions. In *7th International Conference on Learning Representations, ICLR 2019, New Orleans, LA, USA, May 6-9, 2019*. OpenReview.net, 2019.
- [19] Jeff Johnson, Matthijs Douze, and Hervé Jégou. Billion-scale similarity search with GPUs. *IEEE Transactions on Big Data*, 7(3):535–547, 2019.
- [20] K. J. Joseph, Salman Hameed Khan, Fahad Shahbaz Khan, and Vineeth N. Balasubramanian. Towards open world object detection. *2021 IEEE/CVF Conference on Computer Vision and Pattern Recognition (CVPR)*, pages 5826–5836, 2021.
- [21] Jonathan Krause, Michael Stark, Jia Deng, and Li Fei-Fei. 3d object representations for fine-grained categorization. *2013 IEEE International Conference on Computer Vision Workshops*, pages 554–561, 2013.
- [22] A. Krizhevsky and G. Hinton. Learning multiple layers of features from tiny images. *Master’s thesis, Department of Computer Science, University of Toronto*, 2009.
- [23] Yangguang Li, Feng Liang, Lichen Zhao, Yufeng Cui, Wanli Ouyang, Jing Shao, Fengwei Yu, and Junjie Yan. Supervision exists everywhere: A data efficient contrastive language-image pre-training paradigm. *ArXiv*, abs/2110.05208, 2021.
- [24] Norman Mu, Alexander Kirillov, David A. Wagner, and Saining Xie. Slip: Self-supervision meets language-image pre-training. *ArXiv*, abs/2112.12750, 2021.
- [25] Maria-Elena Nilsback and Andrew Zisserman. Automated flower classification over a large number of classes. *2008 Sixth Indian Conference on Computer Vision, Graphics & Image Processing*, pages 722–729, 2008.
- [26] Omkar M. Parkhi, Andrea Vedaldi, Andrew Zisserman, and C. V. Jawahar. Cats and dogs. In *2012 IEEE Conference on Computer Vision and Pattern Recognition, Providence, RI, USA, June 16-21, 2012*, pages 3498–3505. IEEE Computer Society, 2012.
- [27] Pramuditha Perera, Vlad I. Morariu, Rajiv Jain, Varun Manjunatha, Curtis Wigington, Vicente Ordonez, and Vishal M. Patel. Generative-discriminative feature representations for open-set recognition. In *2020 IEEE/CVF Conference on Computer Vision and Pattern Recognition, CVPR 2020, Seattle, WA, USA, June 13-19, 2020*, pages 11811–11820. IEEE, 2020.
- [28] Alec Radford, Jong Wook Kim, Chris Hallacy, Aditya Ramesh, Gabriel Goh, Sandhini Agarwal, Girish Sastry, Amanda Askell, Pamela Mishkin, Jack Clark, Gretchen Krueger, and Ilya Sutskever. Learning transferable visual models from natural language supervision. In Marina

- Meila and Tong Zhang, editors, *Proceedings of the 38th International Conference on Machine Learning, ICML 2021, 18-24 July 2021, Virtual Event*, volume 139 of *Proceedings of Machine Learning Research*, pages 8748–8763. PMLR, 2021.
- [29] Muhammad Imran Razzak, Saeeda Naz, and Ahmad Zaib. Deep learning for medical image processing: Overview, challenges and future. *ArXiv*, abs/1704.06825, 2017.
- [30] Shuhuai Ren, Yihe Deng, Kun He, and Wanxiang Che. Generating natural language adversarial examples through probability weighted word saliency. In *Proceedings of the 57th Annual Meeting of the Association for Computational Linguistics*, pages 1085–1097, Florence, Italy, 2019. Association for Computational Linguistics.
- [31] Shuhuai Ren, Junyang Lin, Guangxiang Zhao, Rui Men, An Yang, Jingren Zhou, Xu Sun, and Hongxia Yang. Learning relation alignment for calibrated cross-modal retrieval. In *Proceedings of the 59th Annual Meeting of the Association for Computational Linguistics and the 11th International Joint Conference on Natural Language Processing (Volume 1: Long Papers)*, pages 514–524, Online, 2021. Association for Computational Linguistics.
- [32] Shibani Santurkar, Dimitris Tsipras, and Aleksander Madry. BREEDS: benchmarks for subpopulation shift. In *9th International Conference on Learning Representations, ICLR 2021, Virtual Event, Austria, May 3-7, 2021*. OpenReview.net, 2021.
- [33] Walter J. Scheirer, Lalit P. Jain, and Terrance E. Boult. Probability models for open set recognition. *IEEE Transactions on Pattern Analysis and Machine Intelligence*, 36:2317–2324, 2014.
- [34] Walter J. Scheirer, Anderson Rocha, Archana Sapkota, and Terrance E. Boult. Toward open set recognition. *IEEE Transactions on Pattern Analysis and Machine Intelligence*, 35:1757–1772, 2013.
- [35] Tongzhou Wang and Phillip Isola. Understanding contrastive representation learning through alignment and uniformity on the hypersphere. In *Proceedings of the 37th International Conference on Machine Learning, ICML 2020, 13-18 July 2020, Virtual Event*, volume 119 of *Proceedings of Machine Learning Research*, pages 9929–9939. PMLR, 2020.
- [36] Mitchell Wortsman, Gabriel Ilharco, Mike Li, Jong Wook Kim, Hannaneh Hajishirzi, Ali Farhadi, Hongseok Namkoong, and Ludwig Schmidt. Robust fine-tuning of zero-shot models. *ArXiv*, abs/2109.01903, 2021.
- [37] Jianxiong Xiao, James Hays, Krista A. Ehinger, Aude Oliva, and Antonio Torralba. SUN database: Large-scale scene recognition from abbey to zoo. In *The Twenty-Third IEEE Conference on Computer Vision and Pattern Recognition, CVPR 2010, San Francisco, CA, USA, 13-18 June 2010*, pages 3485–3492. IEEE Computer Society, 2010.
- [38] Lewei Yao, Runhui Huang, Lu Hou, Guansong Lu, Minzhe Niu, Hang Xu, Xiaodan Liang, Zhenguo Li, Xin Jiang, and Chunjing Xu. Filip: Fine-grained interactive language-image pre-training. *ArXiv*, abs/2111.07783, 2021.
- [39] Ryota Yoshinashi, Wen Shao, Rei Kawakami, Shaodi You, Makoto Iida, and Takeshi Naemura. Classification-reconstruction learning for open-set recognition. In *IEEE Conference on Computer Vision and Pattern Recognition, CVPR 2019, Long Beach, CA, USA, June 16-20, 2019*, pages 4016–4025. Computer Vision Foundation / IEEE, 2019.
- [40] Alireza Zareian, Kevin Dela Rosa, Derek Hao Hu, and Shih-Fu Chang. Open-vocabulary object detection using captions. *2021 IEEE/CVF Conference on Computer Vision and Pattern Recognition (CVPR)*, pages 14388–14397, 2021.
- [41] Renrui Zhang, Rongyao Fang, Wei Zhang, Peng Gao, Kunchang Li, Jifeng Dai, Yu Jiao Qiao, and Hongsheng Li. Tip-adapter: Training-free clip-adapter for better vision-language modeling. *ArXiv*, abs/2111.03930, 2021.
- [42] Kaiyang Zhou, Jingkang Yang, Chen Change Loy, and Ziwei Liu. Learning to prompt for vision-language models. *ArXiv*, abs/2109.01134, 2021.
- [43] Kaiyang Zhou, Jingkang Yang, Chen Change Loy, and Ziwei Liu. Conditional prompt learning for vision-language models. *ArXiv*, abs/2203.05557, 2022.

A Superclass-class hierarchy for vocabulary construction

To construct the vocabulary in § 2, we leverage the underlying superclass-class hierarchical structure of CIFAR100 [22] and ImageNet [6], and group the classes belonging to the same superclass into a vocabulary. Table 2 lists the vocabularies in CIFAR100, which are specified by [22]. There are 20 vocabularies, each with 5 classes. For ImageNet, we utilize two superclass-class structures, Entity13 and Living17, in [32]. Table 3 and Table 4 show the vocabularies in ImageNet (Entity13) and ImageNet (Living17), respectively. The former has 13 vocabularies, each with 20 classes, while the latter has 17 vocabularies, each with 4 classes.

B Dataset-level extensibility

The evaluation protocol in § 2 estimates the extensibility and stability within a single task dataset, where the input images and classes during the vocabulary expansion come from the same data distribution. While the protocol is an approximation of the real open world, current CLIP-like models have exhibited serious performance degradation. In this section, we take a step further toward the real open recognition, by conducting vocabulary expansion setting on the dataset level, where the expanded vocabularies are from different datasets. In this way, the relationship between vocabularies is more uncertain and thus can be viewed as a rigorous stress test for the CLIP-like models. Specifically, we group all categories in a dataset into one vocabulary. Afterward, the inputs and classes of the entire new dataset are introduced at each expansion. Classes in the new vocabulary will be removed if they already exist in the previous vocabularies.

The experiments are conducted with datasets for generic objects, including CIFAR10 [22], CIFAR100 [22], Caltech101 [8], SUN397 [37] and ImageNet [6], and specialized datasets focusing on fine-grained categories, including Flowers102 [25], OxfordPets [26] and StanfordCars [21]. Without loss of the generality, we merge 3 datasets and evaluate the following dataset compositions:

- (1) CIFAR100-Caltech101-SUN397
- (2) CIFAR10-CIFAR100-ImageNet
- (3) Flowers102-OxfordPets-StanfordCars

Composition (1) and (2) probe the performance when all the expanded datasets are generic thus the classes in different datasets are semantics correlated, while composition (3) targets scenarios where the coming datasets have little correlation with previous ones. To eliminate the effect of vocabulary expansion order, we report the average performance of all $A_3^3 = 6$ possible trials for each composition.

Table 5 demonstrates the result of the dataset-level expansion. **First**, the performance of CLIP-like models on generic dataset expansion drops dramatically. For example, the accuracy (Acc-E) of CLIP (RN101) decreases by an averaged absolute point of 14.2 on the *CIFAR100-Caltech101-SUN397* composition during expansion, and 14.5 on the *CIFAR10-CIFAR100-ImageNet* composition, respectively. Due to the existence of subclass-superclass relationship for some classes in different generic datasets, e.g., *cat* in CIFAR10 and *tiger cat* in ImageNet, CLIP is extremely unstable on such expansion considering generic datasets. For example, the Acc-S of CLIP (RN101) on the *CIFAR10-CIFAR100-ImageNet* composition is 28.2% lower than Acc-C, indicating the models are prone to be confused about the subclass-superclass relationship. **Meanwhile**, the CLIP-like models exhibit much better extensibility and stability on the dataset-level expansion considering specialized datasets, e.g., the *Flowers102-OxfordPets-StanfordCar* composition. The vocabularies of this composition are intrinsically disjoint in semantics, so the model can be stably extended. **In summary**, our investigations on the dataset level expansions along with the task level in the paper show the current CLIP-like models fail to meet the expectation of conducting real open vocabulary recognition, and we hope our studies can motivate future studies in this direction.

C Incremental Acc-E and Acc-S on CIFAR100

We record the Acc-E (Eq. 3) and Acc-S (Eq. 6) after each vocabulary expansion on CIFAR100 to investigate the effect of increased task openness on CLIP-like models’ performance.

Table 2: Superclass-class hierarchy in CIFAR100. Each superclass corresponds to a vocabulary, and each vocabulary has 5 classes. There are 20 kinds of vocabulary in total, specified by [22].

Vocabulary (Superclass)	Classes
aquatic	mammals beaver, dolphin, otter, seal, whale
fish	aquarium fish, flatfish, ray, shark, trout
flowers	orchids, poppies, roses, sunflowers, tulips
food	containers bottles, bowls, cans, cups, plates
fruit and vegetables	apples, mushrooms, oranges, pears, sweet peppers
household electrical devices	clock, computer keyboard, lamp, telephone, television
household	furniture bed, chair, couch, table, wardrobe
insects	bee, beetle, butterfly, caterpillar, cockroach
large carnivores	bear, leopard, lion, tiger, wolf
large man-made outdoor things	bridge, castle, house, road, skyscraper
large natural outdoor scenes	cloud, forest, mountain, plain, sea
large omnivores and herbivores	camel, cattle, chimpanzee, elephant, kangaroo
medium-sized mammals	fox, porcupine, possum, raccoon, skunk
non-insect invertebrates	crab, lobster, snail, spider, worm
people	baby, boy, girl, man, woman
reptiles	crocodile, dinosaur, lizard, snake, turtle
small mammals	hamster, mouse, rabbit, shrew, squirrel
trees	maple, oak, palm, pine, willow
vehicles 1	bicycle, bus, motorcycle, pickup truck, train
vehicles 2	lawn-mower, rocket, streetcar, tank, tractor

Figure 10 shows the Acc-E for 20 trials as new vocabularies are merged incrementally. The falling lines indicate that the model is either performing poorly on the new input images, or that some images that were correctly identified before are misclassified after introducing the new classes.

Figure 11 shows Acc-S of CLIP-like models during non-target vocabulary expansion. Each sub-figure represents the situation when one vocabulary is selected as the target vocabulary. As the remaining 19 non-target vocabularies are incorporated and the model is required to recognize the 5 target classes from 100 potential classes, the accuracy drops sharply. The decrease of Acc-S brought by each introduction of non-target vocabulary indicates that more images from the target vocabulary are incorrectly classified into the new non-target vocabulary by models.

D Cosine similarity of image-text features on intact CIFAR100

Figure 12 illustrates the averaged cosine similarity between image and text features of CLIP (ViT-B/32) on all classes of CIFAR100. The elements on the diagonal represent the similarity of the positive image-text pairs, while the others represent that of the negative ones. Since every 5 adjacent classes in the figure constitute a vocabulary (superclass),⁴ the classes belonging to the same vocabulary have higher similarity and smaller margin, which is more likely to be confused with each other.

Our Retrieval-enhanced Prompt Engineering (REPE) method alleviates this issue by enlarging the margin between positive and the largest negative similarity. As shown in Figure 13, the median value of REPE’s margin distribution is .01 (the blue vertical line), which is larger than that of CLIP (ViT-B/32) with .005 (the red line). It indicates that the predictions of REPE are harder to be inverted with competing classes than the original CLIP, thus yielding better performance on the open tasks.

E Quantified loss of inter-modal alignment and intra-modal uniformity

Table 6 provides quantified loss of alignment and uniformity based on Eq. 9 and Eq. 10 defined in § 3.2. CLIP with only cross-modal contrastive learning results in poor intra-modal uniformity. On the vision side, compared with ResNet-101 [14], using a more powerful visual encoder such as ViT [7] can reduce the loss of image uniformity from -0.57 to -0.93 . Besides, the ℓ_{uniform} of SLIP [24]

⁴See Table 2 in Appendix A.

Table 3: Superclass-class hierarchy in ImageNet (Entity13). Each superclass corresponds to a vocabulary, and each vocabulary has 20 classes. There are 13 kinds of vocabulary in total, specified by BREEDS [32].

Vocabulary (Superclass)	Classes
garment	trench coat, abaya, gown, poncho, military uniform, jersey, cloak, bikini, miniskirt, swimming trunks, lab coat, brassiere, hoopskirt, cardigan, pajama, academic gown, apron, diaper, sweatshirt, sarong
bird	African grey, bee eater, coucal, American coot, indigo bunting, king penguin, spoonbill, limpkin, quail, kite, prairie chicken, red-breasted merganser, albatross, water ouzel, goose, oystercatcher, American egret, hen, lorikeet, ruffed grouse
reptile	Gila monster, agama, triceratops, African chameleon, thunder snake, Indian cobra, green snake, mud turtle, water snake, loggerhead, sidewinder, leatherback turtle, boa constrictor, garter snake, terrapin, box turtle, ringneck snake, rock python, American chameleon, green lizard
arthropod	rock crab, black and gold garden spider, tiger beetle, black widow, barn spider, leafhopper, ground beetle, fiddler crab, bee, walking stick, cabbage butterfly, admiral, lacewing, trilobite, sulphur butterfly, cicada, garden spider, leaf beetle, long-horned beetle, fly
mammal	Siamese cat, ibex, tiger, hippopotamus, Norwegian elkhound, dugong, colobus, Samoyed, Persian cat, Irish wolfhound, English setter, llama, lesser panda, armadillo, indri, giant schnauzer, pug, Doberman, American Staffordshire terrier, beagle
accessory	bib, feather boa, stole, plastic bag, bathing cap, cowboy boot, necklace, crash helmet, gasmask, maillot, hair slide, umbrella, pickelhaube, mit- ten, sombrero, shower cap, sock, running shoe, mortarboard, handkerchief
craft	catamaran, speedboat, fireboat, yawl, airliner, container ship, liner, trimaran, space shuttle, aircraft carrier, schooner, gondola, canoe, wreck, warplane, balloon, submarine, pirate, lifeboat, airship
equipment	volleyball, notebook, basketball, hand-held computer, tripod, projector, barbell, monitor, croquet ball, balance beam, cassette player, snorkel, horizontal bar, soccer ball, racket, baseball, joystick, microphone, tape player, reflex camera
furniture	wardrobe, toilet seat, file, mosquito net, four-poster, bassinet, chiffonier, folding chair, fire screen, shoji, studio couch, throne, crib, rocking chair, dining table, park bench, chest, window screen, medicine chest, barber chair
instrument	upright, padlock, lighter, steel drum, parking meter, cleaver, syringe, abacus, scale, corkscrew, maraca, saltshaker, magnetic compass, accordion, digital clock, screw, can opener, odometer, organ, screwdriver
man-made structure	castle, bell cote, fountain, planetarium, traffic light, breakwater, cliff dwelling, monastery, prison, water tower, suspension bridge, worm fence, turnstile, tile roof, beacon, street sign, maze, chain-link fence, bakery, drilling platform
wheeled vehicle	snowplow, trailer truck, racer, shopping cart, unicycle, motor scooter, passenger car, minibus, jeep, recreational vehicle, jinrikisha, golfcart, tow truck, ambulance, bullet train, fire engine, horse cart, streetcar, tank, Model T
produce	broccoli, corn, orange, cucumber, spaghetti squash, butternut squash, acorn squash, cauliflower, bell pepper, fig, pomegranate, mushroom, strawberry, lemon, head cabbage, Granny Smith, hip, ear, banana, artichoke

Table 4: Superclass-class hierarchy in ImageNet (Living17). Each superclass corresponds to a vocabulary, and each vocabulary has 4 classes. There are 17 kinds of vocabulary in total, specified by BREEDS [32].

Vocabulary (Superclass)	Classes
salamander	eft, axolotl, common newt, spotted salamander
turtle	box turtle, leatherback turtle, loggerhead, mud turtle
lizard	whiptail, alligator lizard, African chameleon, banded gecko
snake	night snake, garter snake, sea snake, boa constrictor
spider	tarantula, black and gold garden spider, garden spider, wolf spider
grouse	ptarmigan, prairie chicken, ruffed grouse, black grouse
parrot	macaw, lorikeet, African grey, sulphur-crested cockatoo
crab	Dungeness crab, fiddler crab, rock crab, king crab
dog	bloodhound, Pekinese, Great Pyrenees, papillon
wolf	coyote, red wolf, white wolf, timber wolf
fox	grey fox, Arctic fox, red fox, kit fox
domestic cat	tiger cat, Egyptian cat, Persian cat, Siamese cat
bear	sloth bear, American black bear, ice bear, brown bear
beetle	dung beetle, rhinoceros beetle, ground beetle, long-horned beetle
butterfly	sulphur butterfly, admiral, cabbage butterfly, ringlet
ape	gibbon, orangutan, gorilla, chimpanzee
monkey	marmoset, titi, spider monkey, howler monkey

Table 5: Extensibility and stability of CLIP and its variants during dataset-level vocabulary expansion. Δ refers to the decline of Acc-E/Acc-S (%) compared to Acc-C (%). PE denotes Prompt Ensemble.

Model	CIFAR100-Caltech101-SUN397					CIFAR10-CIFAR100-ImageNet					Flowers102-OxfordPets-StanfordCars				
	Acc-C	Extensibility		Stability		Acc-C	Extensibility		Stability		Acc-C	Extensibility		Stability	
		Acc-E	Δ	Acc-S	Δ		Acc-E	Δ	Acc-S	Δ		Acc-E	Δ	Acc-S	Δ
CLIP (RN101)	65.9	51.7	-14.2	52.7	-13.2	62.4	47.9	-14.5	34.2	-28.2	65.8	63.1	-2.7	65.7	-0.1
CLIP (ViT-B/32)	72.0	59.4	-12.6	61.2	-10.8	70.9	52.7	-18.2	41.3	-29.6	65.8	62.0	-3.8	65.8	-0.0
CLIP (ViT-B/16)	74.6	60.6	-14.0	61.7	-12.9	74.7	56.6	-18.0	43.3	-31.4	72.3	69.6	-2.7	72.3	-0.0
SLIP (ViT-B/16)	58.6	44.4	-14.2	46.3	-12.3	55.6	36.7	-18.9	30.5	-25.1	35.0	26.0	-9.0	35.0	-0.0
DeCLIP (ViT-B/32)	74.3	60.8	-13.5	63.3	-11.0	73.0	55.4	-17.6	45.1	-27.9	70.2	63.3	-6.9	70.2	-0.0
PE (ViT-B/32)	71.8	59.9	-11.9	59.6	-12.2	72.2	53.5	-18.7	41.6	-30.6	65.7	62.0	-3.7	65.7	-0.0
PE (ViT-B/16)	75.0	61.5	-13.5	62.5	-12.5	75.4	56.7	-18.7	41.3	-34.1	72.5	70.0	-2.5	72.5	-0.0

Table 6: Inter-modal alignment (ℓ_{align}), text uniformity ($\ell_{\text{uniform-T}}$), image uniformity ($\ell_{\text{uniform-I}}$), Acc-C (Eq. 4), and Acc-E (Eq. 3) of CLIP-like models on CIFAR100. For the first three metrics, lower numbers are better. For the last two metrics, higher numbers are better.

Model	Alignment & Uniformity			Accuracy	
	ℓ_{align} (\downarrow)	$\ell_{\text{uniform-T}}$ (\downarrow)	$\ell_{\text{uniform-I}}$ (\downarrow)	Acc-C (\uparrow)	Acc-E (\uparrow)
CLIP (RN101)	1.15	-1.16	-0.57	68.3	55.4
CLIP (ViT-B/32)	1.48	-0.96	-0.93	78.0	69.6
CLIP (ViT-B/16)	1.50	-0.97	-0.81	79.7	72.6
SLIP (ViT-B/16)	1.73	-2.86	-1.69	63.9	51.1
DeCLIP (ViT-B/32)	1.62	-2.96	-1.87	78.7	70.8
PE (ViT-B/32)	1.46	-0.96	-0.93	78.3	70.3
PE (ViT-B/16)	1.48	-0.97	-0.81	79.6	72.6
CoOp (ViT-B/16)	1.40	-3.16	-0.81	83.6	76.9

Table 7: Instances of the captions retrieved by our REPE on CIFAR100.

Class	Retrieved captions
apple	“Apple slices stacked on top of each other”
	“Apples growing on a tree”
	“Still life with apples in a basket”
woman	“Portrait of a young woman”
	“Woman standing at the window”
	“Confident woman in a red dress and gold crown”
bridge	“The golden bridge in Bangkok”
	“Bridge on the River Kwai ~Video Clip”
	“Wooden bridge over a mountain river”
ray	“Stingray in the Grand Cayman, Cayman Islands stock photography”
	“Common Stingray swimming close to the sea floor.”
	“Sun Rays Tours: Go Pro captured the rays under water”

Table 8: A comparison of Closed Set Recognition, Open Set Recognition (OSR), Open World Recognition, and Open-vocabulary Recognition (OVR).

Task	Paradigm	Goal	Signal	Training	Testing
Closed Set Recognition	Classification	Identifying known classes	Supervised	Known classes	Known classes
Open Set Recognition	Classification	Identifying known classes & rejecting unknown classes	Supervised	Known classes	Known classes & unknown classes
Open World Recognition	Classification	Identifying known classes & detecting unknown classes & labeling unknown data & incrementally learn and extend classifier	Supervised	Incremental known classes	Known classes & unknown classes
Open-vocabulary Recognition	Matching	Identifying classes via natural language	Unsupervised	-	Classes in a vocabulary

and DeCLIP [23] is much lower than CLIP, indicating their better intra-modal uniformity derived by intra-modal contrastive learning in pre-training, which enforces both image and text features separate better from classes. As for the prompt tuning [42] method (CoOp), it achieves better ℓ_{align} compared to CLIP and the lowest $\ell_{\text{uniform-T}}$ of -3.16 .

F Case study of retrieved caption in REPE

Table 7 shows some cases of the captions retrieved by our proposed REPE on CIFAR100. They share the same target of interest with the original prompt, i.e., “a photo of a [CLASS]”, but provide the context in which the class name is located and thus have richer semantics. For example, given a class like *bridge*, the retrieved captions describe its possible properties (e.g., “golden”, “wooded”), connections to other objects (e.g., “over a mountain river”), etc., yielding more expressive and distinguishable text features of the class. However, REPE also recalls some low-quality captions. For example, given the class *ray*, a large, flat sea fish with a long, narrow tail, in CIFAR100, the caption “Sun Rays Tours: Go Pro captured the rays under water” is retrieved, where the “ray” in the caption refers to a narrow beam of light, heat, etc. We leave the retrieval with better semantics preservation for future work.

G Comparison of related work

Table 8 provides a more detailed comparison of Closed Set Recognition, Open Set Recognition (OSR) [34, 11], Open World Recognition (OWR) [1], and Open-vocabulary Recognition (OVR) [28] from 5 perspectives paradigm, goal, signal, classes type in training, and classes type in testing, respectively. Contrary to other research, the CLIP-based Open-vocabulary Recognition is unsupervised. We focus on the model performance on zero-shot inference, without training or fine-tuning on the target dataset.

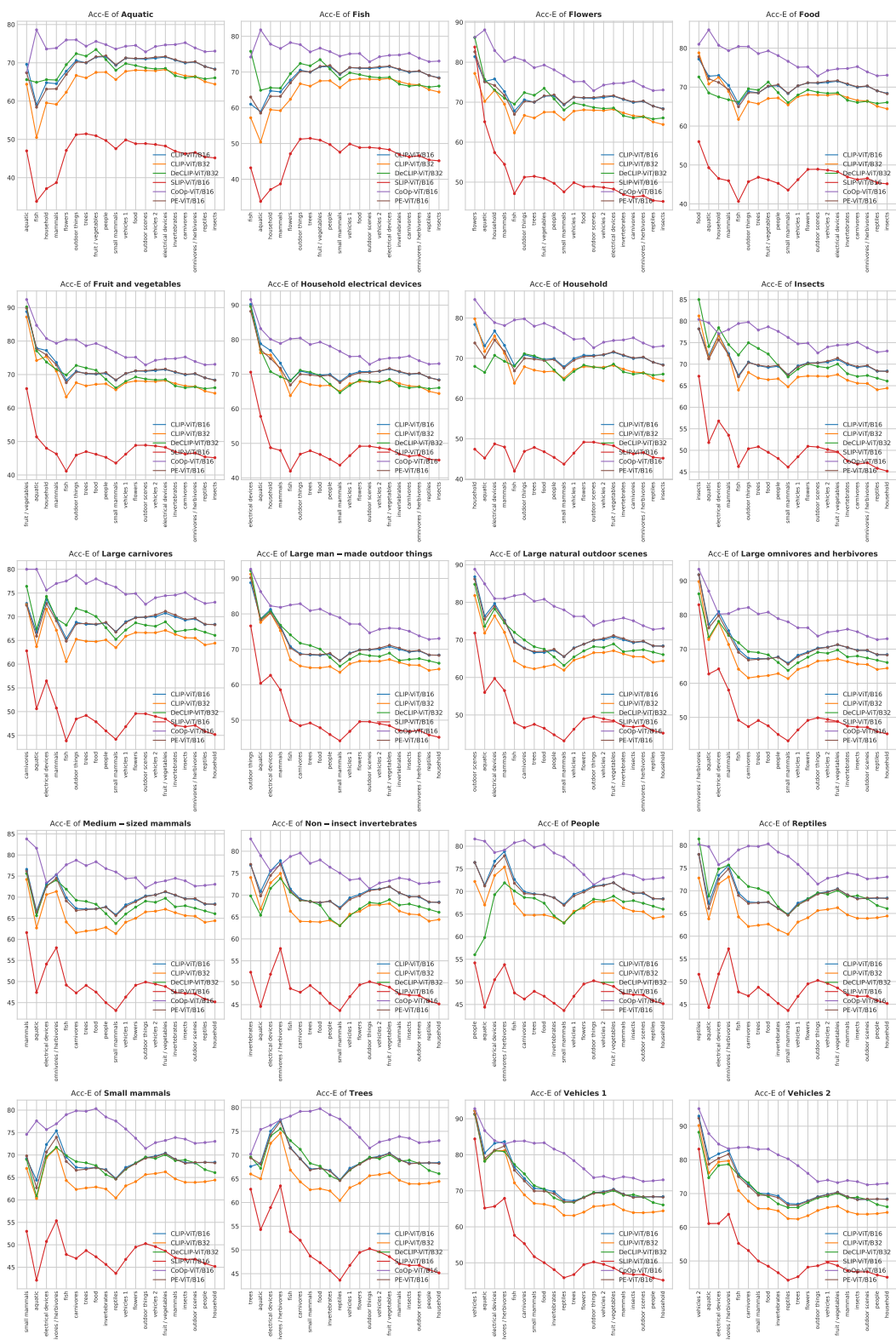


Figure 10: Incremental Acc-E of CLIP and its variants on CIFAR100.

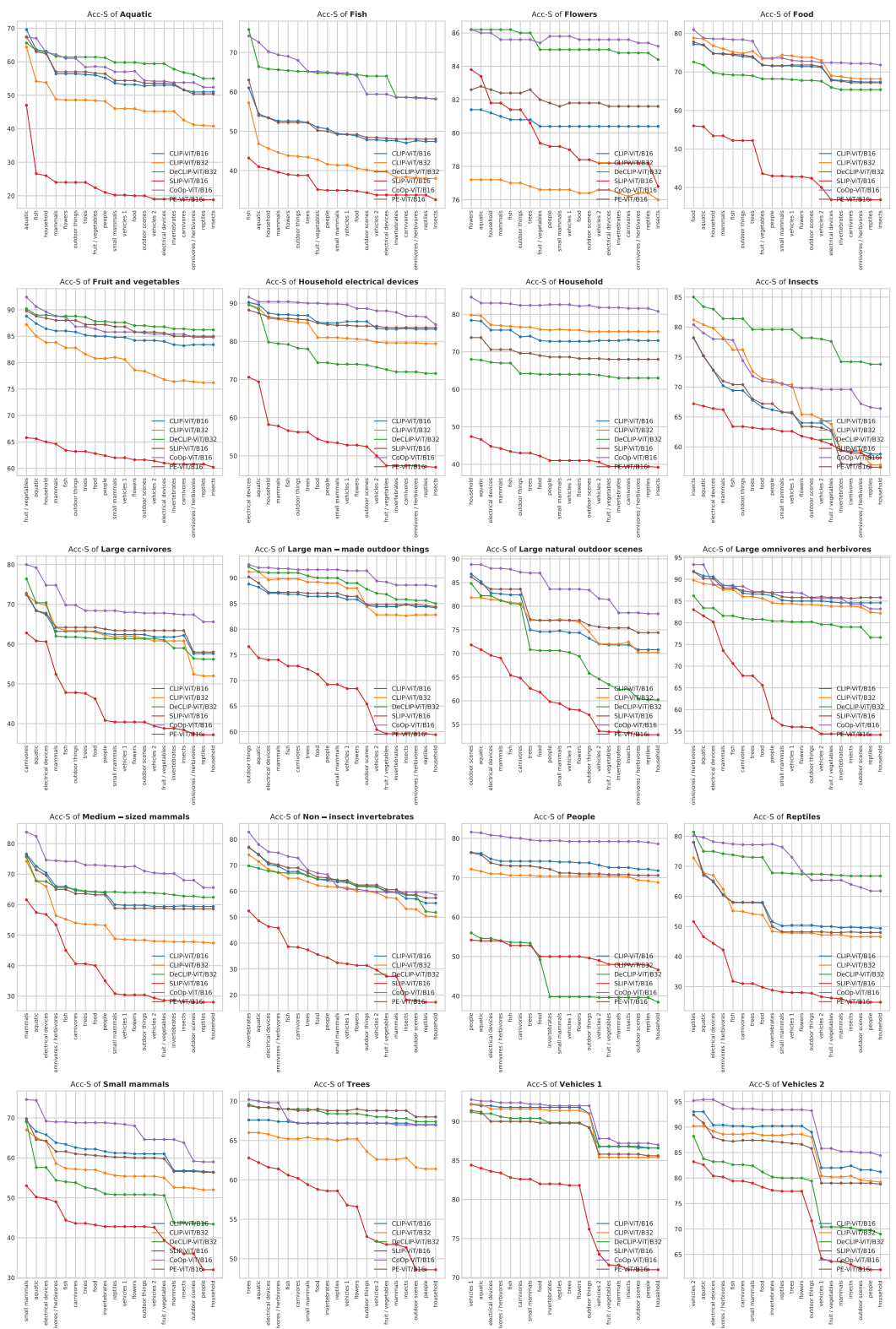


Figure 11: Incremental Acc-S of CLIP and its variants on CIFAR100.

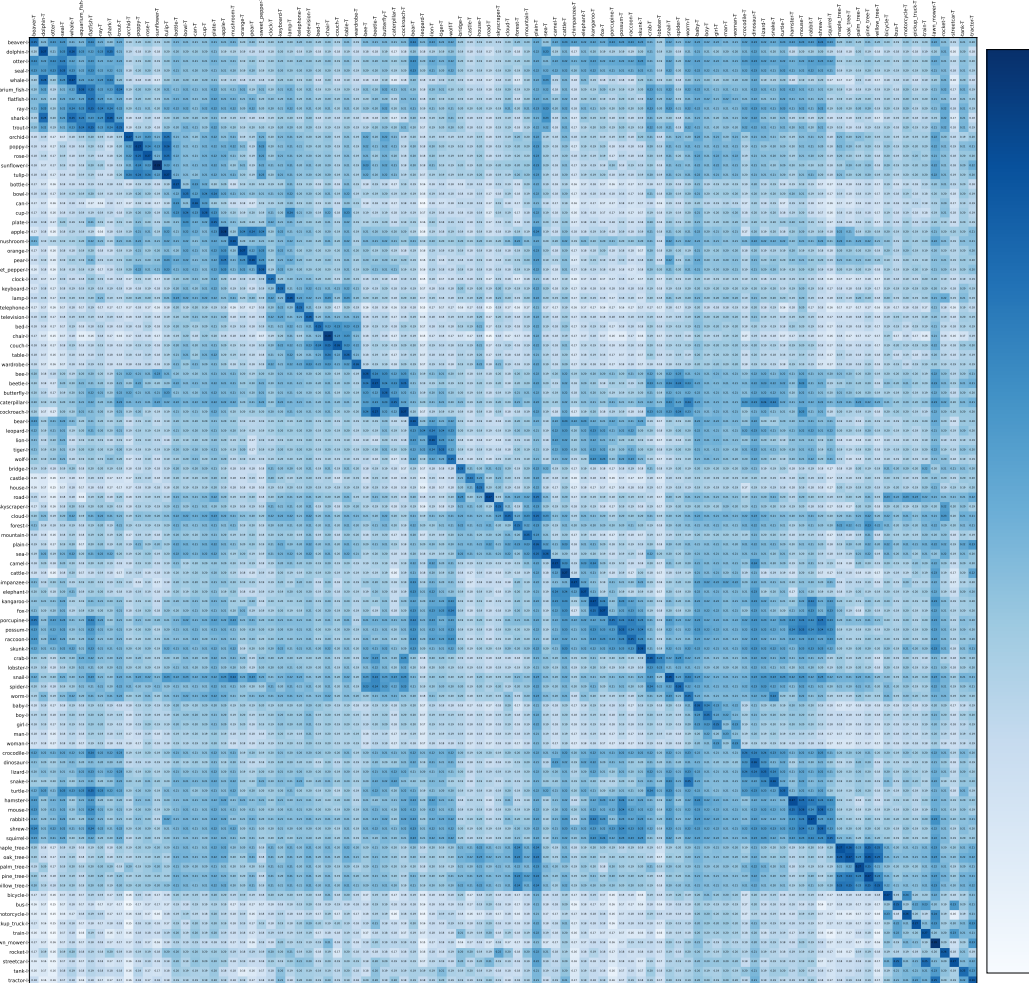


Figure 12: Averaged cosine similarity between image (-I) and prompt (-T) features of CLIP (ViT-B/32) on intact CIFAR100. The elements on the diagonal represent the similarity of the positive image-text pairs, while the others represent that of the negative ones.

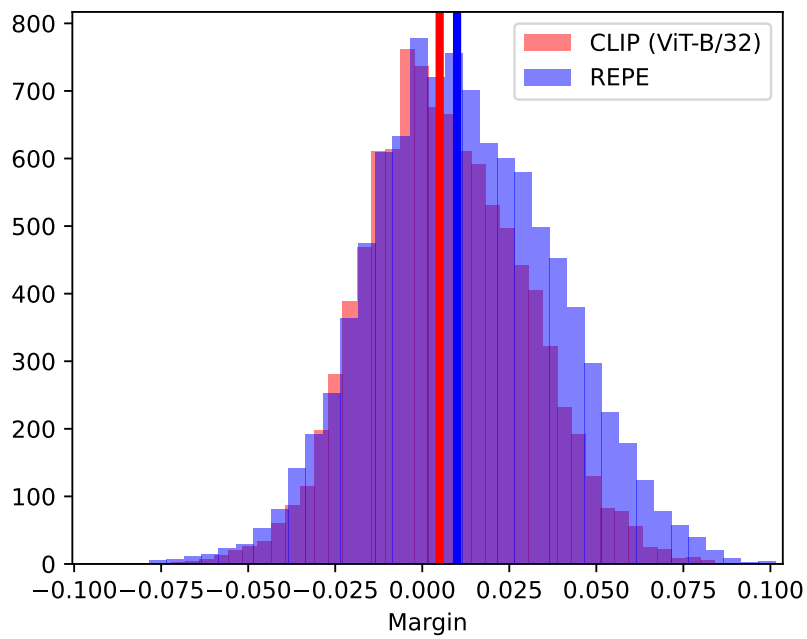


Figure 13: Margin distribution of similarity scores of our REPE (blue) and CLIP (ViT-B/32) (red). The median value of REPE’s distribution is .01 (the blue vertical line), which is larger than that of CLIP (ViT-B/32) with .005 (the red line). It indicates that the predictions of REPE are harder to be inverted with competing classes than the original CLIP.